

The role of groundwater in the Amazon water cycle: 3. Influence on terrestrial water storage computations and comparison with GRACE

Yadu N. Pokhrel,¹ Ying Fan,¹ Gonzalo Miguez-Macho,² Pat J.-F. Yeh,³
and Shin-Chan Han⁴

Received 26 October 2012; revised 11 March 2013; accepted 14 March 2013; published 30 April 2013.

[1] We explore the mechanisms whereby groundwater influences terrestrial water storage (TWS) in the Amazon using GRACE observations and two contrasting versions of the LEAF-Hydro-Flood hydrological model: one with and the other without an interactive groundwater. We find that, first, where the water table is shallow as in northwestern Amazonia and floodplains elsewhere, subsurface stores (vadose zone and groundwater) are nearly saturated year-round, hence river and flooding dominate TWS variation; where the water table is deep as in southeastern Amazonia, the large subsurface storage capacity holds the infiltrated water longer before releasing it to streams, hence the subsurface storage dominates TWS variation. Second, over the whole Amazon, the subsurface water contribution far exceeds surface water contribution to total TWS variations. Based on LEAF-Hydro-Flood simulations, 71% of TWS change is from subsurface water, 24% from flood water, and 5% from water in river channels. Third, the subsurface store includes two competing terms, soil water in the vadose zone and groundwater below the water table. As the water table rises, the length of vadose zone is shortened and hence the change in groundwater store is accompanied by an opposite change in soil water store resulting in their opposite phase and contributions to total TWS. We conclude that the inclusion of a prognostic groundwater store and its interactions with the vadose zone, rivers, and floodplains in hydrological simulations enhances seasonal amplitudes and delays seasonal peaks of TWS anomaly, leading to an improved agreement with GRACE observations.

Citation: Pokhrel, Y. N., Y. Fan, G. Miguez-Macho, P. J.-F. Yeh, and S.-C. Han (2013), The role of groundwater in the Amazon water cycle: 3. Influence on terrestrial water storage computations and comparison with GRACE, *J. Geophys. Res. Atmos.*, 118, 3233–3244, doi:10.1002/jgrd.50335.

1. Introduction

[2] This paper is the third part of a series of three companion papers on the role of groundwater in the Amazon water cycle. In part 1, *Miguez-Macho and Fan* [2012a] gave a literature synthesis on the mechanisms whereby groundwater regulates seasonal dynamics of surface waters from headwater streams to the large floodplains. They also described LEAF-Hydro-Flood (hereafter referred to as LHF), an integrated, continental-scale land hydrology model (details under

section 4). It includes a prognostic groundwater interacting with soils, rivers, and wetlands within a grid cell, and lateral groundwater convergence among cells; it solves the full momentum equation in routing river and over-bank flooding also allowing backwater effects; it also ties land drainage with the sea level. This model was applied to the Amazon at 2 km, 4 min resolution for 11 years (2000–2010), forced by European Centre for Medium-Range Weather Forecasts Interim Reanalysis. Results were compared with observed daily discharge at the 10 largest gauges, seasonal water table depth at eight sites, and satellite-observed seasonal flooding. The model was used to test four groundwater hypotheses. First, in headwater catchments of the Amazon, groundwater is the dominant source of streamflow, but the proportion varies due to varying water table depth; a shallow water table limits infiltration, enhancing saturation-excess runoff. Second, in the lower floodplains, two-way exchange occurs between the floodwater and the groundwater; in wet seasons, rain and expanding floodwater infiltrate into floodplain sediments, the amount controlled by water table depth; in dry seasons, the flow reverses, and groundwater seeps out to feed floodplain lakes and wetlands. Third, groundwater supports wetlands rarely

¹Department of Earth and Planetary Sciences, Rutgers University, New Brunswick, New Jersey, USA.

²Non-Linear Physics Group, Faculty of Physics, Universidade de Santiago de Compostela, Galicia, Spain.

³International Centre for Water Hazard and Risk Management (ICHARM) under the auspices of UNESCO, Tsukuba, Japan.

⁴Planetary Geodynamics Laboratory, NASA Goddard Space Flight Center, Greenbelt, Maryland, USA.

Corresponding author: Y. N. Pokhrel, Department of Earth and Planetary Sciences, Rutgers University, New Brunswick, NJ 08854, USA. (yadupokhrel@eps.rutgers.edu)

flooded but characterized by a persistently shallow water table, creating water-logged conditions defining wetlands. Fourth, the longer time scales of groundwater delay and dampen river flow and flooding; because of its slow response to rainfall, groundwater seeps may peak and persist in the dry season. The four mechanisms were observed in isolated sites across the Amazon, and we provided a model synthesis/assessment of their basin-scale significance. Two parallel simulations, LHF vs. fixed-depth (4 m) soil without groundwater, highlight the difference that groundwater makes. Our results underscore the damping effect of groundwater where it is deep (storing excess rainfall in wet season and releasing in dry season) and the accelerating effect where it is shallow (enhancing surface saturation and quick runoff).

[3] In part 2, *Miguez-Macho and Fan* [2012b] evaluated groundwater's role in modulating seasonal soil moisture and evapotranspiration (ET). A known model-data disagreement is the dry-season water stress; while models suggest water limitation, observations suggest little difference between wet- and dry-season ET. We reviewed field literature on the possible mechanisms for the lack of water stress, and posted four hypotheses on groundwater influence. First, a shallow water table can be a direct source for plant uptake in the extensive wetlands and flooded forests in central Amazon. Second, a shallow water table impedes wet-season drainage, leading to larger soil water stores at the beginning of the dry season and giving the plants a strong start. Third, a shallow water table can send up capillary rise to the root zone. Fourth, due to its delayed and dampened response to seasonal rainfall, the timing of groundwater can buffer dry season stress; across the Amazon, it has been shown that the water table reaches its seasonal peak weeks to months after the peak seasonal rainfall, and the surplus or deficit in groundwater stores from one season can carry over to the next. Furthermore, the temporal delay also manifests itself as spatial patterns; throughout the dry season, continued drainage and convergence from high grounds sustains a shallow water table in the valleys, keeping them moist all year round and forming a structured mosaic of wet-dry patches, supporting dry-season ET at least in the lower parts of the landscape. After comparing our simulation with observed interception loss at two sites, soil moisture at seven deep pits, and ET at six flux towers, we tested these hypotheses by contrasting two simulations, LHF vs. fixed-depth (4 m) soil without groundwater. The findings support these hypotheses suggesting groundwater contributions to maintaining Amazon ecosystems.

[4] In this study, part 3 of the series, we investigate how groundwater may contribute to the variations in terrestrial water storage (TWS). Following a similar approach as in parts 1 and 2, we explore the mechanisms whereby groundwater may regulate TWS variations, and contrast the results of two parallel simulations, LHF vs. fixed-depth (4 m) soil without groundwater.

2. Terrestrial Water Storage and GRACE

[5] Terrestrial water storage, which is composed of water stored above and underneath the land surface, influences the Earth system through multiple pathways. Near the surface, soil water controls ET and hence water-energy exchange

between the land surface and the atmosphere, directly affecting the physical climate; by limiting ET, soil water availability affects land ecosystem dynamics and the associated carbon and nutrient fluxes, indirectly affecting the climate; immediately below, the shallow phreatic groundwater feeds streams, lakes, and wetlands, modulating land aquatic ecosystems and carbon fluxes; further down, groundwater storage in the aquifers provides vital support for water and food (via irrigation) security in societies on arid and semiarid lands. In high altitudes and polar regions, changes in ice mass have direct impact on seasonal streamflow and sea level change [e.g., *Luthcke et al.*, 2006; *Chen et al.*, 2009b, 2011]. Lastly, seasonal water loading and the resulting crustal deformation have been evoked to explain the seasonality in volcanism [e.g., *Mason et al.*, 2004], which, through gas and particle emissions, further feeds back to the climate system. Thus, understanding the changes in TWS and the contributions to total TWS variations from different hydrologic stores (snow and ice, soil water, groundwater, river, and flood water) can provide key insights into the hydrologic cycle and its response-feedback to the Earth's climate system.

[6] The GRACE satellite mission [*Tapley et al.*, 2004], operational since mid-2002, provides a unique opportunity to monitor TWS from space [*Rodell and Famiglietti*, 2002; *Wahr et al.*, 2004]. The monthly gravity field solutions obtained from the twin-satellites can be used to estimate the vertically integrated water storage variations with a resolution of a few hundred kilometers, and at a precision of a few centimeters of water depth [*Swenson et al.*, 2003; *Rodell et al.*, 2004; *Chambers*, 2006]. Because the seasonal changes in the hydrologic cycle are among the strongest GRACE signals, numerous studies have exploited the opportunity to study TWS variations over large river basins [*Hirschi et al.*, 2006; *Yeh et al.*, 2006; *Seo et al.*, 2006; *Klees et al.*, 2007; *Han et al.*, 2009; *Kim et al.*, 2009; *Pokhrel et al.*, 2012]. Among these studies, there has been a particular interest in the Amazon basin [e.g., *Crowley et al.*, 2008; *Chen et al.*, 2009a, 2010; *Han et al.*, 2009, 2010; *Xavier et al.*, 2010; *Becker et al.*, 2011] because it exhibits the largest annual TWS signal observed by GRACE [*Tapley et al.*, 2004] and the amount of water stored and flowing through its extensive forests and floodplains is still poorly constrained [*Alsdorf et al.*, 2010].

[7] In addition to direct TWS monitoring, GRACE data are also used to evaluate TWS simulated by global and continental-scale models [e.g., *Niu and Yang*, 2006; *Kim et al.*, 2009; *Han et al.*, 2009; *Syed et al.*, 2008; *Hirschi et al.*, 2006; *Alkama et al.*, 2010; *Ngo-Duc et al.*, 2007; *Lo et al.*, 2010; *Werth and Güntner*, 2010; *Pokhrel et al.*, 2012]. In this context, GRACE provides the "ground truth" for the models, and the models provide means to partition the vertically integrated TWS observed by GRACE into contributing components such as atmospheric, canopy, soil, snow-ice, surface, and subsurface water. These studies demonstrated a general model-GRACE agreement on TWS changes, although the models tend to have smaller seasonal amplitudes [e.g., *Niu et al.*, 2007; *Ngo-Duc et al.*, 2007] and earlier responses to rainfall forcing [*Pokhrel et al.*, 2012; *Alkama et al.*, 2010]. Regarding the partition of TWS into contributing hydrologic stores, there is little agreement; e.g., *Kim et al.* [2009] suggested that river storage explains ~73% of TWS variation in the Amazon, while *Alkama et al.*

[2010] suggested that TWS variation in the Amazon is almost equally partitioned into soil moisture and river storage variations. *Han et al.* [2010] also found that the soil moisture storage from Land Surface Model Simulations driven by the Global Land Data Assimilation System contributes to TWS over the Amazon by ~50% and the rest of it is explained by the storage computed through lateral runoff routing, which also lumped the movement of shallow groundwater. Their study showed large spatial variations in seasonal TWS changes. In the Rio Negro, *Frappart et al.* [2008] suggested that surface and subsurface water equally contribute to TWS variations, but their recent study [*Frappart et al.*, 2011] shows that groundwater contributes up to ~72% in the downstream reaches of the Negro basin.

[8] The disagreement could be partially due to the differences in approaches that the models treat groundwater. Most land surface models either do not have a groundwater store—the drainage from the fixed-depth (typically 2–4 m) soil column is directly placed into river store—or parameterize a simple groundwater holding tank as a passive receiver of soil drainage with a calibrated, delayed release to rivers. In the study of *Kim et al.* [2009], deep soil drainage is placed into the river store which effectively lumps the variation of groundwater store resulting in the large contribution of river store (~73%) to total TWS variation. River contribution was reduced in the studies with a groundwater holding tank [e.g., *Alkama et al.*, 2010; *Ngo-Duc et al.*, 2007]. *Niu et al.* [2007] further showed that groundwater variation explains most of the TWS signal in the Amazon when a simple dynamic groundwater store is considered.

[9] The goal of this study is to shed further lights on groundwater's role in modulating TWS in the Amazon. Our fully coupled groundwater-surface model may offer new insights for the following reasons. First, the model groundwater is fully prognostic with explicit mass balance and two-way flux exchange with soils, rivers, and floodplains. Second, it allows not only vertical, within grid-cell, interactions with soil, river, and floodplain, but also lateral groundwater convergence among grid cells from high to low grounds; this lateral convergence has long time scales and can affect the rainfall residence time in a basin. Third, the simulation is performed at a high spatial resolution (2 km), resolving large changes in water table depth; across the Amazon, the mean water table can vary from the land surface to >50 m deep, and the seasonal rise and fall at a site can be >15 m; this large spatial-temporal variability in water table depth is well documented in field observations across the Amazon (see review in *Miguez-Macho and Fan* [2012a]), and it suggests a large soil and groundwater storage capacity where the water table is deep (more room to rise and fall) and small capacity where it is shallow (near saturation). This is an advantage over current large-scale modeling studies. Fourth, allowing backwater in river and floodwater movement slows down river discharge and increases residence time. Lastly, allowing floodwater to infiltrate into the sediments under the vast floodplains of the Amazon and seeping out at low water further delays the discharge into the ocean. Intuitively, these processes are likely to influence the amplitude and timing of TWS changes; they are explicitly represented in LHF. Furthermore, tests with available observations of river discharge, water table depth, flooding, soil moisture, and ET flux [*Miguez-Macho and Fan*, 2012a, 2012b] have

placed constraints on the physical realism of LHF. We also note that no model parameters are calibrated to match the observations. In these respects, a study using LHF may contribute new insights into the ongoing investigations of Amazon TWS.

3. Mechanisms Whereby Groundwater Regulates TWS Variations

[10] We propose that groundwater regulates seasonal TWS variations through several mechanisms, labeled as M-1 to M-6 in Figure 1. It illustrates a topographic sequence with nested rivers (low- to high-order streams from left to right) and a multiscale groundwater flow system whereby recharge in a given model cell can enter the stream within the cell (M-2) or the stream in the lower neighbor via downslope groundwater flow (M-3). Where the water table is at the land surface such as at the base of slopes (M-4), rainfall cannot infiltrate into the soil and will runoff the land and enter the nearest stream. It also shows a floodplain at the lower end of the multiscale drainage system, where the floodwater can infiltrate into the floodplain sediments and return to the streams at the low river stage (M-5). Model representation is also shown (dashed lines) with the mean grid elevation (grey) and water table depth (green). This hydrologic conceptualization is supported by a large number of field observations in the Amazon reviewed by *Miguez-Macho and Fan* [2012a, 2012b].

[11] In nature, the water table depth varies from being deep under the hills as in cell-A (Figure 1) to near or at the land surface in the lower valleys as in cell C, that is, the vadose zone depth, and storage capacity, can vary from cell to cell. This fact is captured in Figure 2, a 7 year (overlapping with GRACE data used here) mean seasonal water table depth, simulated by LHF [*Miguez-Macho and Fan*, 2012a, 2012b] and validated with water table, soil moisture, ET, river discharge and flooding observations. In the southern and eastern Amazon, the water table varies between 5–80 m under the hills, but remains shallow in the valleys. It also remains perennially shallow in large regions in the northwestern Amazon (<2.5 m). This large variability of vadose zone length, in both space and time, cannot be captured by modeling approaches using a uniformly fixed soil column depth shown in red in Figure 1, which includes only a small fraction of the vadose zone in cell A, but the water table or part of the groundwater store in cell C. In nature, soil infiltration in cell-A must reach the water table before it enters the stream, while in a model with a fixed-depth soil, drainage from the base is instantly placed in the river. In cell A, the longer vadose zone and transit time through this zone increase soil water store and retain it for longer time than it would be with a short and fixed-depth soil column. This vadose zone delay is well documented; across the Amazon, it has been shown that under the high grounds, the water table reaches its seasonal peak weeks to months after the peak seasonal rainfall [*Hodnett et al.*, 1997a, 1997b; *Johnson et al.*, 2006; *Grogan and Galvão*, 2006; *Cuartas*, 2008; *Vourlitis et al.*, 2008; *Tomasella et al.*, 2008]. This long vadose zone transit time effectively delays the discharge of soil water into the rivers, increases the volume of vadose zone store, and hence affects the timing and amplitude of its contributions to TWS variations. This is the first mechanism whereby a

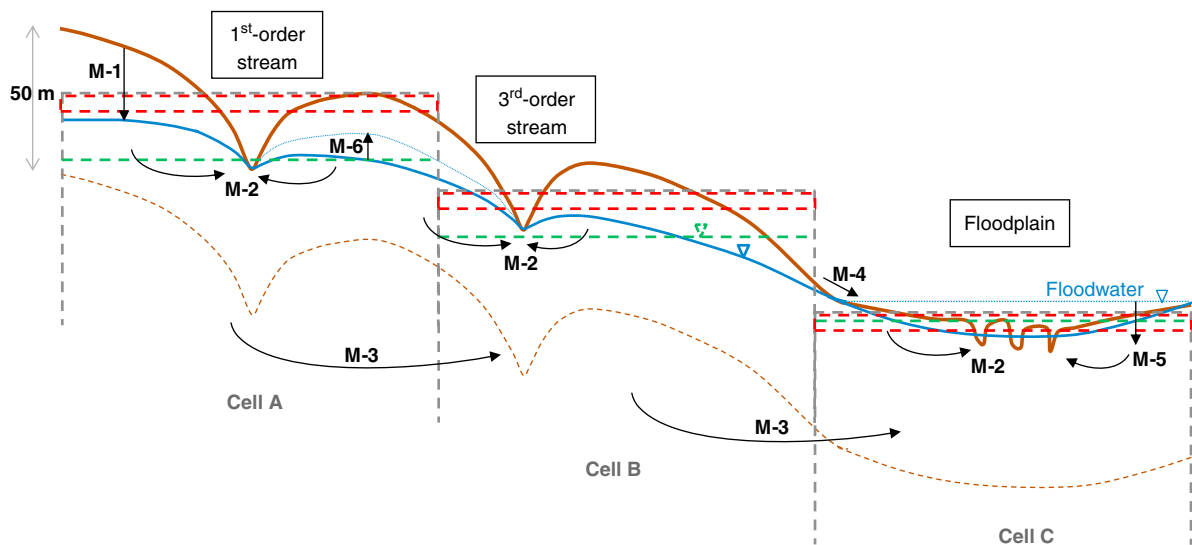


Figure 1. Schematic of the groundwater system in the Amazon (solid lines) where the water table (blue) intercepts the valley floor (brown) feeding local streams (M-2), and the local hydraulic gradient is superimposed on a regional gradient resulting in groundwater outflow bypassing local stream outlet into lower valleys (M-3). Model representation is also shown (dashed lines) with grid mean elevation (grey) and water table depth (green). The dashed red box indicates the uniformly fixed-depth soil column in standard land models. The thin dashed brown line indicates 50 m below land surface; groundwater storage is the volume of water above it and below the water table (solid blue). The proposed six mechanisms whereby groundwater affects TWS are labeled as M-1 to M-6.

prognostic groundwater can influence TWS variations (M-1, Figure 1).

[12] The second mechanism (M-2, Figure 1) stems from the fact that in nature (and simulated in LHF) the rate of groundwater discharge into streams is determined by the water level difference between the two stores and their hydraulic connection, the latter being a function of groundwater-surface water contact area (controlled by water table height and drainage density) and soil permeability. That is, there is a resistance between groundwater store and river store. Hence the infiltration reaching the water table at a given time step may leave the system much later, often long after the recharge event. This mechanism effectively holds the groundwater in the subsurface longer, increasing its storage and delaying its release, which will affect the magnitude and timing of TWS and groundwater contributions.

[13] The third mechanism (M-3, Figure 1) is related to the fact that in nature groundwater can leave a catchment without passing through the river outlet, as already shown theoretically [Toth, 1963; Schaller and Fan, 2009] and observed in the headwater catchments of the Amazon [Lesack, 1993; Neu et al., 2011]. Neu et al. [2011] reported that in a headwater catchment of Xingu, 88% of total runoff is groundwater outflow through the deeply weathered soils bypassing the river outlet. Multiscale groundwater flow is captured in LHF, allowing cell-to-cell groundwater flow governed by head differences among cells and soil permeability (per Darcy's law), so that groundwater in cell A can discharge into streams in cell B or even cell C (Figure 1). Because lateral groundwater convergence is slow, the transit time can be long, holding groundwater even longer in the system and further delaying its discharge into rivers.

[14] The fourth mechanism (M-4, Figure 1) is that the shallow water table, near or at the land surface, impedes soil

infiltration and enhances saturation-excess overland runoff (Dunn runoff mechanism) during rainfall events. As shown in Figure 2 and observed throughout the Amazon (Brazilian Geological Survey as compiled in Fan and Miguez-Macho [2010]; Bongers et al. [1985]; Poels [1987]; Lesack [1995]; Coomes and Grubb [1996]; Hodnett et al. [1997a, 1997b]; McClain et al. [1997]; Selhorst et al. [2003]; Grogan and Galvão [2006]; Jirka et al. [2007]; Tomasella et al. [2008]; Cuartas [2008]; Vourlitis et al. [2008]; Borma et al. [2009]; Lähteenoja and Page [2011]; Neu et al. [2011]), the water table is ubiquitously shallow under the valleys and floodplains. Thus, in the areas where the water table is shallow before rainy season as in the northwestern Amazon (Figure 2, SON), subsurface store is nearly saturated and hence surface store has to absorb most of the incoming rainfall, explaining a large portion of TWS variations here. Models without the shallow water table to limit infiltration would predict more infiltration and less surface runoff, underestimating surface water contributions to TWS.

[15] The fifth mechanism (M-5, Figure 1) lies under the extensive floodplains. As floodwater tops the river banks and spreads laterally, it infiltrates into the yet unsaturated sediments below. It stays there until the river stage has fallen and the slow seepage into the floodplain rivers, and lakes drains it down, as documented by field studies across the Amazon [Forsberg et al., 1988; Mertes, 1997; Lesack, 1995; Lesack and Melack, 1995; Cullmann et al., 2006; Hamilton et al., 2007; Bonnet et al., 2008; Borma et al., 2009; Bourrel et al., 2009]. This floodplain storage, termed bank storage [e.g., Winter et al., 1998], converts surface water into groundwater once more before the rivers enter the sea, and it effectively holds on to the water longer and increases groundwater store. As shown earlier [Miguez-Macho and Fan, 2012a], the floodplain

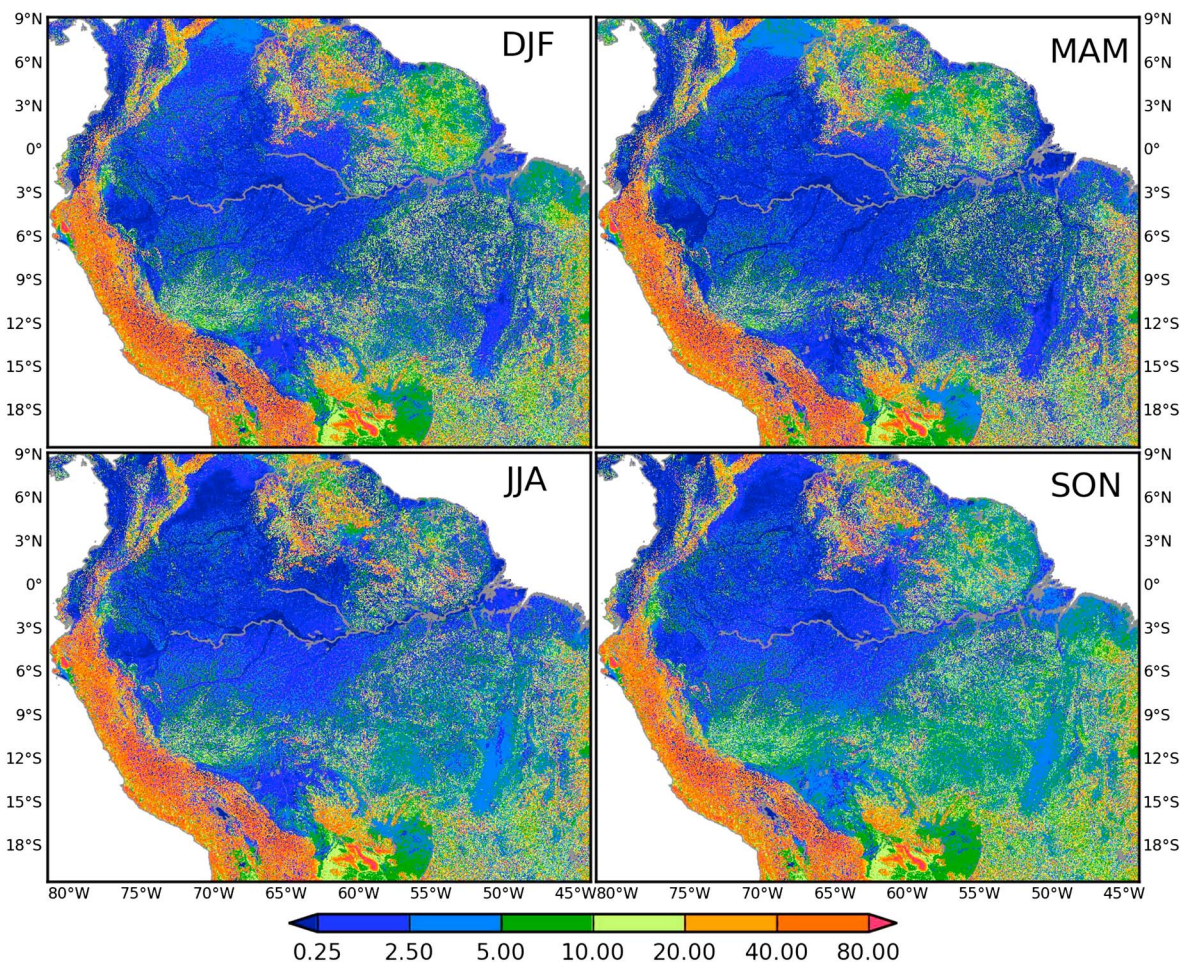


Figure 2. LEAF-Hydro-Flood simulated, 2004–2010 mean, seasonal water table depth (meters below land surface) (Details in *Miguez-Macho and Fan [2012a, 2012b]*), where DJF is December to February, MAM is March to May, JJA is June to August, and SON is September to November.

infiltration loss can be significant at the five largest floodplains in the Amazon.

[16] Lastly (M-6, cell A, Figure 1), as the water table rises in response to recharge, it invades the vadose zone and shortens the unsaturated column; hence, an increase in groundwater store is necessarily accompanied by a decrease in soil water store. The competition between the saturated and unsaturated stores in the subsurface is known [*Duffy, 1996*], but models without a dynamic water table cannot represent this fact. Often TWS studies in the literature demonstrate a rise and fall of soil water store synchronous to seasonal rainfall.

[17] The combined effect of mechanisms 1, 2, 3, and 5 is to delay the discharge (TWS peak shifted later) and increase storage (enhanced amplitude of TWS anomaly), while mechanism 4 does the opposite by enhancing surface runoff, a quick process of shedding water. Mechanism 6 leads to an opposite-phase change between vadose zone and groundwater stores, challenging current views of soil water contribution to TWS from large-scale model-GRACE comparison studies. These mechanisms are accounted for in LHF and we expect to see their influences on the simulated TWS. We note that our river routing scheme, which slows and even reverses flow at large river junctions by accounting

for backwater effects of low-gradient rivers, also serves to hold the water longer in the rivers and floodplains, but because it is not directly related to groundwater processes, we will not include it here as one of the mechanisms. In light of these mechanisms, in the following we examine the TWS variations as simulated LHF, referred to as the LHF-experiment, and a parallel simulation with a fixed 4 m deep soil column, free soil drainage at the base, and immediate placement of runoff into the river store within the cell, referred to as the FD-experiment, to bring out the influence of groundwater. We then compare both simulations with GRACE observations.

4. Methods

[18] We use the coupled groundwater-surface water model LHF. For brevity, only key processes represented in LHF are highlighted here; the readers are referred to the references cited herein for more details. Figure 3 illustrates the model components and their interactions. The standard LEAF (Land Ecosystem-Atmosphere Feedback) [*Walko et al., 2000*] is the land model of the Regional Atmosphere Modeling System, color-coded orange in Figure 3. LEAF-Hydro [*Fan et al., 2007; Miguez-Macho et al., 2007*], color-coded blue in Figure 3, added a prognostic

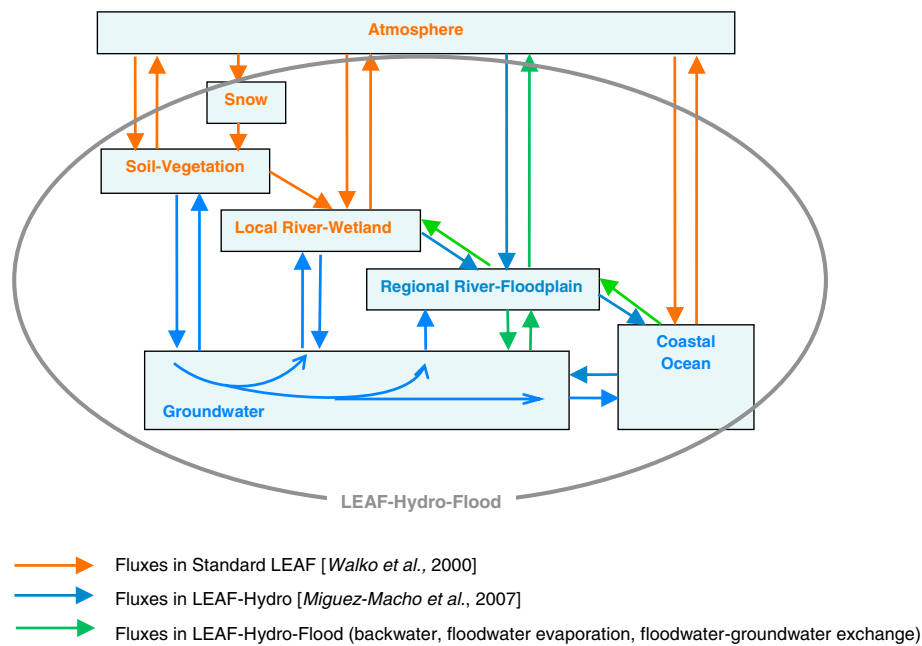


Figure 3. Stores and fluxes included in standard LEAF (orange color-coding) and other typical land models, LEAF-Hydro (blue color-coding), and LEAF-Hydro-Flood (green color-coding).

groundwater store allowing (1) the water table to rise and fall or the vadose zone to shrink or grow; (2) the water table, recharged by infiltration, to relax through discharge into rivers within a grid cell, as well as lateral groundwater flow among adjacent cells, leading to divergence from high grounds and convergence to low valleys at multiple scales; (3) two-way exchange between groundwater and rivers depending on hydraulic difference and river-groundwater contact area, representing both losing (leaking to groundwater) and gaining (receiving groundwater convergence) streams; (4) river discharge routing to the ocean through the channel networks as kinematic waves; and (5) setting the sea level as the groundwater head boundary condition, hence allowing sea level to influence coastal drainage. In our recent Amazon study [Miguez-Macho and Fan, 2012a], we introduced a river-floodplain routing scheme that solves the full momentum equation of open channel flow, taking into account the backwater effect (the diffusion term) [e.g., Yamazaki et al., 2011] and the inertia of large water mass of deep flow (acceleration terms) [e.g., Bates et al., 2010] that are important in the Amazon. This causes the river discharge to be influenced by river stage downstream or the sea level, slowing down or even reversing flow locally. This last development results in the LHF, color-coded green in Figure 3. The model has been extensively tested with observed water table depth, river discharge, seasonal flooding [Miguez-Macho and Fan, 2012a], soil moisture, and ET [Miguez-Macho and Fan, 2012b], over an 11 year (2000–2010) simulation of the Amazon at 4 min time steps and 1 arc-min grids (~2 km), forced by European Centre for Medium-Range Weather Forecasts Reanalysis Interim Product (ERA-Interim). We refer the reader to parts 1 and 2 for details in literature review of groundwater processes in the Amazon, model formulations, parameter estimations, forcing data bias assessment, and model comparisons with observations in both surface and subsurface stores.

[19] We define the following:

Terrestrial Water Storage (TWS) = Surface water + Sub-surface water

Surface water = FW + RW

Subsurface water = VW + GW

where,

FW = water on the floodplains

RW = water in the river channels

VW = soil water in the vadose zone (unsaturated store)

GW = groundwater (below the water table, saturated store)

[20] The GW store is the amount of water from the water table down to 50 m below land surface (Figure 1, between solid blue line and dashed brown line). Because the focus is on its seasonal change rather than the absolute value, the choice of the reference depth (50 m) here is inconsequential.

[21] Subsurface water is partitioned by the water table into two components: soil water in the vadose zone (VW) above and groundwater in the saturated zone (GW) below. As infiltration reaches the water table, GW rises into the vadose zone, causing VW to decrease. If the water table continues to rise and reaches the land surface, VW may completely vanish resulting in no contribution to TWS variations. When such a condition prevails for a prolonged period of time, such as in lowland swamps, total subsurface water store changes little, while large variations occur in surface water stores which have to absorb the continued rainfall and flooding. Conversely, when there is less or no recharge to groundwater in dry season, or if the capillary rise, river discharge and lateral divergence exceed recharge, the water table is lowered, which causes the vadose zone to expand and results in increased VW. This causes variation in both VW and GW, but one component gains water at

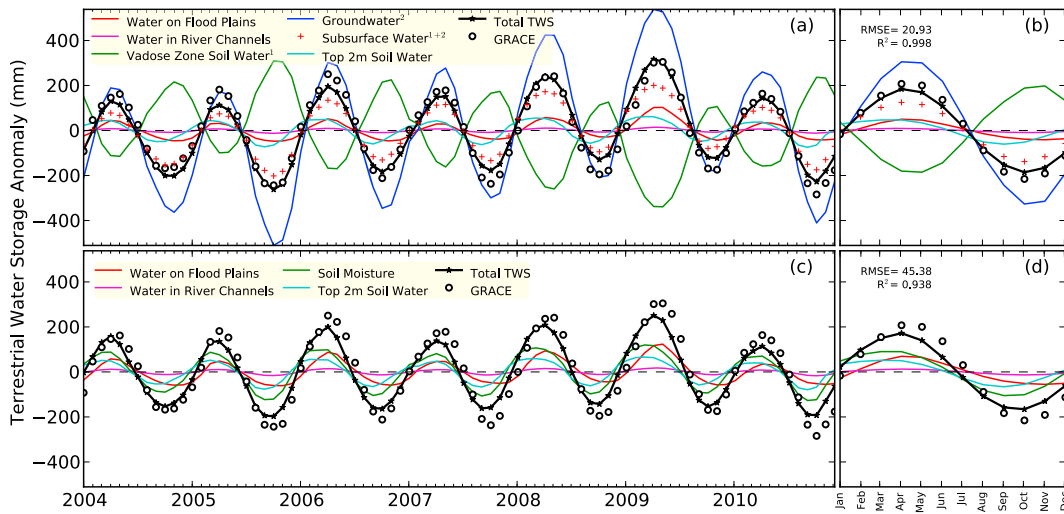


Figure 4. Time series of TWS anomalies averaged over the Amazon basin from the (a) LHF experiment and (c) FD experiment, and (b and d) their seasonal cycles. There is no groundwater storage in the FD experiment. For the GW experiment the net subsurface water (i.e., vadose zone water + groundwater) is also shown (red + signs). All values are shown as water depth in mm.

the expense of the other. Therefore, VW and GW compete with each other for space and evolve over time in opposite phase thus showing a direct but inverse relationship between them [Duffy, 1996]. In this sense, it is more meaningful to consider VW+GW as a whole, and hence we define it as the total subsurface storage.

[22] We note that VW is not identical to soil moisture in conventional land models where the soil column is fixed to a certain depth, typically of 2–4 m from the land surface. To avoid confusion and to make our result comparable to previous studies, we also calculate the water in the top 2 m of soil which is generally assumed to include the plant root zone. We will refer to this storage as the root-zone water, which is only a fraction of the total vadose zone where the water table is deep, and includes groundwater where the water table is shallow. We note that in the FD experiment, there is no explicit groundwater store, and the free-drainage from the 4 m deep soil column is placed immediately into the rivers in the cell. Therefore, the total subsurface water store in the FD experiment is only the soil water in the entire soil column of 4 m depth.

[23] The TWS from the GRACE measurements is the total vertically integrated water stored above and beneath the Earth’s surface. We use the RL05, the latest, $1^\circ \times 1^\circ$ monthly GRACE products provided by the Center for Space Research at the University of Texas at Austin [available at <http://grace.jpl.nasa.gov/data/gracemonthlymassgridsland/>]. The monthly products of the equivalent water height were scaled by using the scaling factors provided with the data to restore much of the energy removed by the de-striping and filtering process [Landerer and Swenson, 2012]. Because the GRACE data (RL05) are available for the period of 2004 to mid-2012 and our simulations span for 2000–2010, we use 2004–2010 as our analysis period for which GRACE and the model overlap. To compare with GRACE, we aggregate model outputs from the original 1 arc min (~ 2 km) grid daily output to $1^\circ \times 1^\circ$ products. Then, the basin-wide averages of both GRACE and model results are obtained by using $1^\circ \times 1^\circ$ river basin masks. For analyses without

GRACE, we use model output at the original ~ 2 km grids and daily time steps.

5. Results and Discussions

[24] Figure 4 shows the comparison of TWS anomaly averaged over the entire Amazon basin, as monthly time series and mean seasonal cycle, and for both LHF and FD experiments. In the LHF experiment (Figures 4a and 4b), the total TWS is partitioned into FW, RW, VW, and GW, while in the FD experiment (Figures 4c and 4d) it is partitioned into FW, RW, and the water in the entire 4 m soil column (VW). GRACE data are shown as circles. We make the following observations.

[25] First, the most prominent feature in the LHF experiment is that the VW (green) varies in opposite phase with GW (blue) due to the mechanism 6 (M-6, Figure 1). Second, the VW (green) in the LHF run has a very large seasonal amplitude compared to the FD run (green), mainly due to the long soil columns (M-1) in LHF in eastern Amazon (deep water table). Third, GW (blue) has the largest seasonal swing due to the large vadose zone in the deep water table regions (M-1), allowing ample rooms for the water table to rise and fall. Fourth, the net effect of the large but opposite-phase changes in VW and GW is expressed in the total subsurface water (red-cross symbol), which is in phase with seasonal rainfall anomalies; the top 2 m root-zone water in LHF (aqua) is comparable to its counterpart in FD (aqua), giving the familiar seasonal patterns reported in earlier model studies. However, this same 2 m store is conceptually different between LHF and FD: in LHF it is wetter containing both VW and GW where the water table is < 2 m deep as in western Amazon, and it is drier containing only VW where the water table is > 2 m deep as in southeastern Amazon, while in FD it is simply the total water content in the top 2 m soil. Fifth, there is a smaller river and floodplain (purple and red) storage change in LHF compared to FD, due to the larger subsurface storage capacity in LHF (from M-1, M-2, M-3, and M-5).

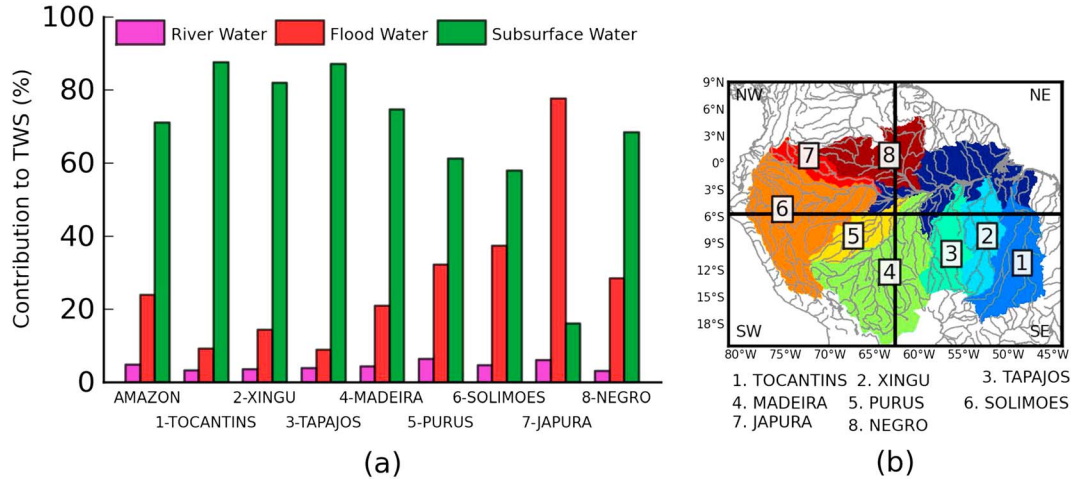


Figure 5. (a) Contribution of different terrestrial water storage components to the total TWS variation averaged over the entire Amazon and the sub-basins, and (b) location of the Amazon and the sub-basins simulated by LEAF-Hydro-Flood. Dark blue indicates the regions in the Amazon which are not covered by the sub-basins, and the four boxes (SW, SE, NE, and NW) show the four quarters selected for the analysis in Tables 1 and 2.

[26] The larger subsurface storage capacity and the slow nature of water movement in the subsurface are the key reasons why LHF gives a seasonal TWS variation closer to GRACE observations in both timing and the amplitude. This is not only reflected graphically, but also quantitatively in root mean square error and R^2 values. The root mean square error in LHF (shown in Figure 4b) is less than half of that in FD (Figure 4d), and the R^2 value is also improved. However, the seasonal amplitude of LHF is still smaller than GRACE, attributed to the well-recognized bias of reduced seasonality in rainfall forcing from ERA-Interim [Betts *et al.*, 2009; Miguez-Macho and Fan, 2012a, 2012b]. Perhaps direct comparison with GRACE is less informative than contrasting LHF and FD runs; in the FD run, the same rainfall forcing bias leads to even smaller amplitude.

[27] We also give a more detailed analysis of the amplitude and timing of LHF and FD vs. GRACE, for the entire Amazon and the four quarters of the model domain (Figure 5b). We examine the four quarters because of the large variability in TWS dynamics across the Amazon, and in particular the northern/southern seasonal off set; the Amazon basin-wide TWS lumps together wet season in some places with dry season in others. Moreover, we selected the four quarters instead of the sub-basins because some of the basins are too small to use GRACE data with the desired accuracy. Table 1 gives the minimum/maximum TWS anomaly

by LHF, FD, and GRACE over the Amazon and the four quarters. For the models, we used daily climatology over the 7 years of overlap with GRACE, and for GRACE, only monthly values are resolved. Model differences from GRACE are shown in parentheses. The mean absolute error over the four quarters (last row) suggests that TWS minimum, maximum and amplitude by LHF are closer to GRACE than that by FD, consistent with what we see with the whole Amazon basin (second last row of Table 1 and Figure 4).

[28] Table 2 evaluates the timing of modeled TWS. It shows the days when the seasonal TWS anomaly changes its sign from positive to negative (the falling limb) and vice versa (the rising limb), over the four quarters and the whole Amazon. For the models the days in the year are identified. For GRACE we assume that its monthly values occur on the 15th day, and that the rising and falling limb near the crossing can be represented as straight lines. Model differences from GRACE are shown in parentheses. The mean absolute error of the four quarters (last row) suggests that LHF gives a closer timing to GRACE than FD does, again consistent with what we see over the whole Amazon basin (second last row in Table 2 and Figures 4b and 4d).

[29] We examine the spatial variability in the mechanisms of TWS change in different parts of the Amazon by further breaking down the Amazon into eight sub-basins. Figure 5a depicts the relative contributions of RW (purple), FW (red),

Table 1. Minimum, Maximum, and Amplitude of TWS Anomaly Simulated by LHF and FD and Observed by GRACE

Quarter		Minimum TWS			Maximum TWS			Amplitude (max-min)		
		LHF	FD	GRACE	LHF	FD	GRACE	LHF	FD	GRACE
1	SW	-174(-38)	-154(-17)	-137	196(65)	194(63)	131	371(103)	347(80)	268
2	SE	-221(-14)	-181(26)	-207	246(28)	203(-14)	217	466(42)	385(-39)	424
3	NE	-183(40)	-164(59)	-223	170(-74)	150(-94)	244	353(-114)	314(-153)	467
4	NW	-70(2)	-85(-13)	-72	102(6)	134(39)	95	172(4)	219(51)	168
Entire Amazon		-189(26)	-171(44)	-215	191(-16)	175(-32)	207	380(-43)	346(-77)	423
Mean abs. error of 4 quarters		23	29		44	52		66	81	

Numbers in parentheses show the difference between model and GRACE.

Table 2. Timing of the Change in Sign of TWS Anomaly Simulated by LHF and FD and Observed by GRACE

Quarters		Julian Day of Change in TWS from Negative to Positive			Julian Day of Change in TWS from Positive to Negative		
		LHF	FD	GRACE	LHF	FD	GRACE
1	SW	10(15)	0(5)	-5	189(11)	172(-6)	178
2	SE	-1(-3)	-19(-21)	2	181(1)	160(-20)	180
3	NE	70(5)	48(-17)	65	253(11)	238(-4)	242
4	NW	107(-2)	89(-20)	109	261(7)	244(-10)	254
Entire Amazon		20(0)	8(-12)	20	203(-1)	188(-16)	204
Mean abs. error of 4 quarters		6	16		8	10	

Numbers in parentheses show the difference between model and GRACE.

and total subsurface water (VW plus GW, green) to TWS variations in the entire Amazon and the sub-basins (Figure 5b). We show the contribution of total subsurface water storage, rather than separating groundwater from vadose zone water, because the amplitude of either can be larger than total TWS being opposite in phase; considering them as a whole is more

meaningful. To calculate the component contributions, first the months of maximum and minimum amplitude of total TWS anomaly, m_1 and m_2 , respectively, are determined, then the component contribution (CC) of each storage term S is calculated for each sub-basin as the ratio of change in component amplitude to the change in total TWS amplitude,

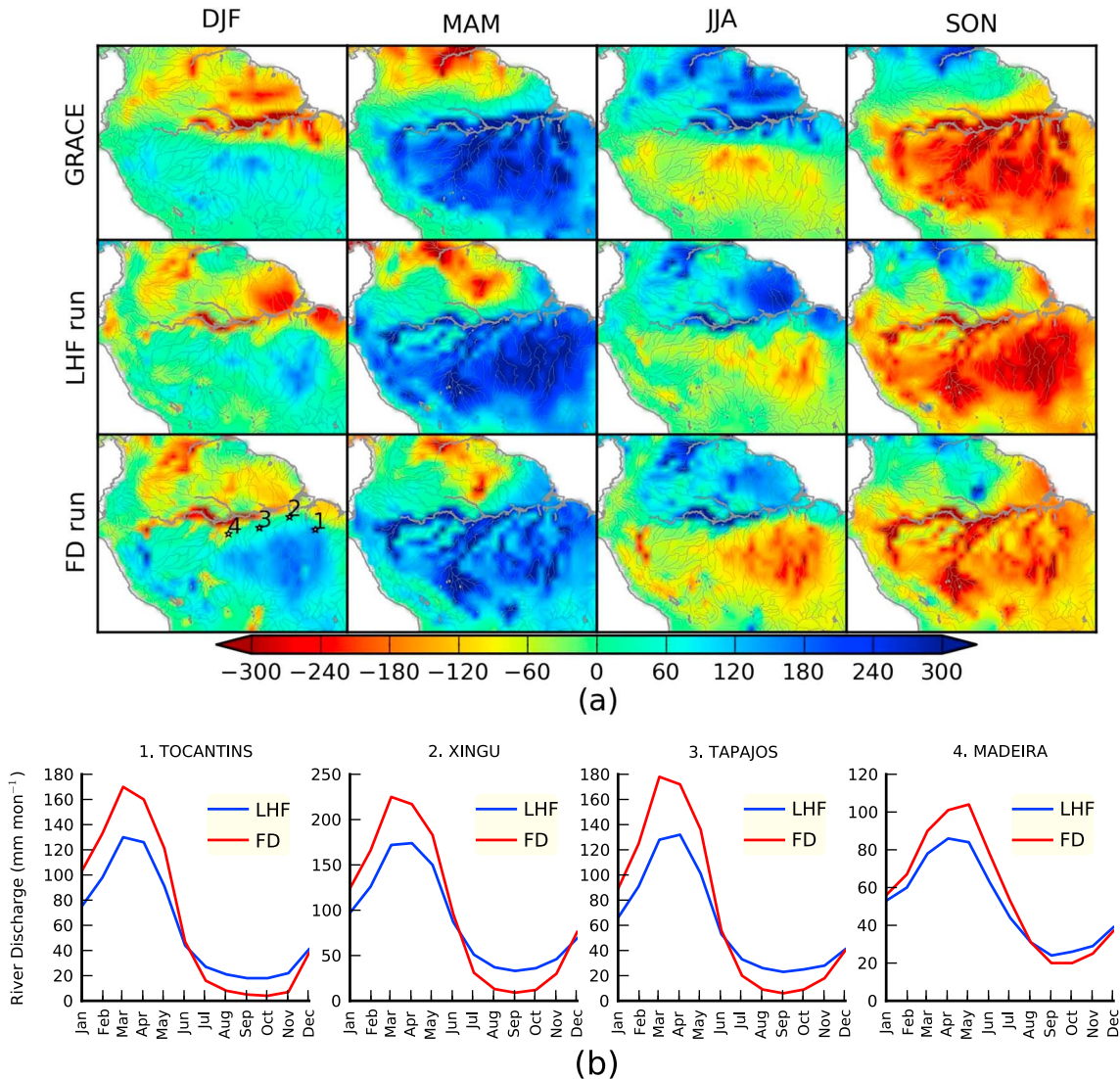


Figure 6. (a) Spatial variations in seasonal TWS anomalies (mm). Results shown are the seasonal averages of the deviation of monthly TWS from the long term (2004–2010) mean TWS. (b) Comparison of river discharge from LEAF-Hydro-Flood (LHF) and free drainage (FD) runs at the gauging stations shown in the lower left panel in Figure 6a. For locations of the basins see Figure 5b.

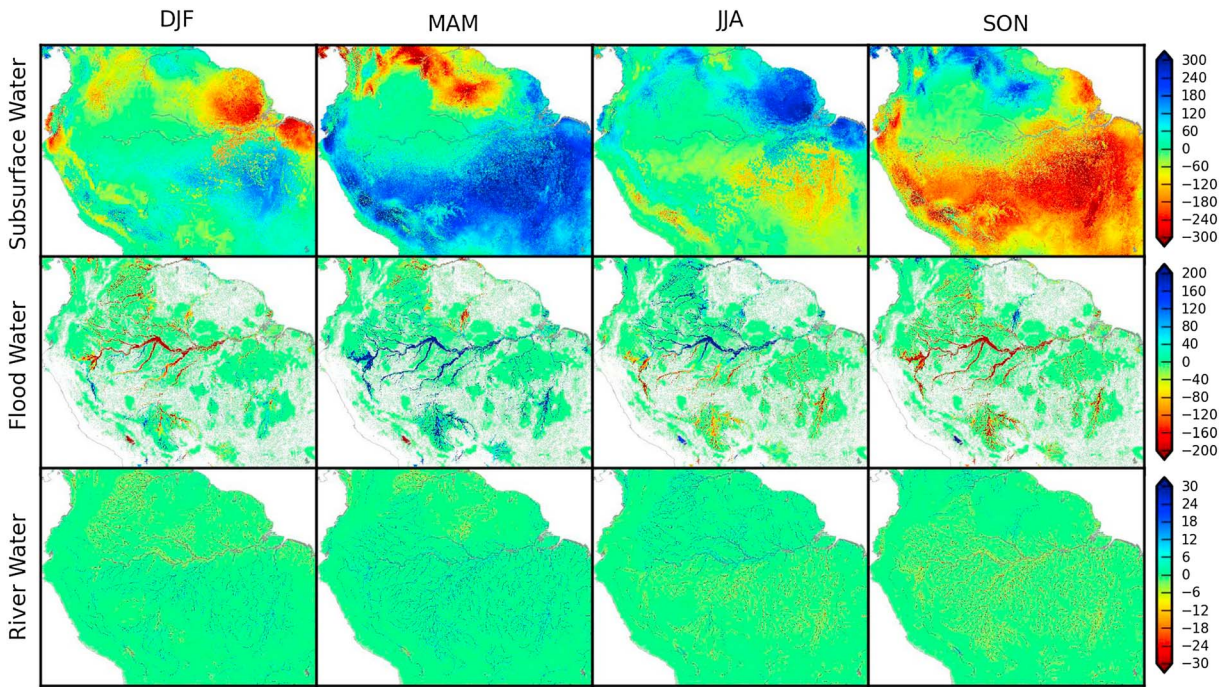


Figure 7. LEAF-Hydro-Flood simulated long-term seasonal anomalies of different TWS components (mm) at the original ~ 2 km model grids. Note that the ranges of color bars differ among the plots.

$$CC_s = (S_{m1} - S_{m2}) / (TWS_{m1} - TWS_{m2})$$

[30] Over the western and northern Amazon where the water table is perennially shallow (5-Purus, 6-Solimoes, 7-Japura, and 8-Negro; water table < 2.5 m deep; Figure 2) and infiltration is impeded, saturation-excess runoff widely occurs, explaining the large floodwater contribution to TWS. Over the southern and eastern Amazon, where the water table is deep particularly before the wet season onset (1-Tocantins, 2-Xingu, 3-Tapajos, and 4-Madeira; water table 5–40 m deep; Figure 2), subsurface stores dominate TWS due to the larger subsurface storage capacity. Over the Amazon as a whole, 71% of TWS change is due to subsurface water, 24% due to flood water, and 5% due to water confined within river channels.

[31] Figure 6a further explores the spatial variations in TWS from GRACE (top), LHF (middle), and FD (bottom) with more spatial details than sub-basins. Where surface water stores are important (shallow water table and nearly saturated subsurface stores), as along the main channels and over the large floodplains, both LHF and FD reproduced well the seasonal changes observed by GRACE, but where subsurface water stores dominate (deep water table and large vadose zone), as in the southeastern Amazon, LHF is closer to GRACE observations. The large subsurface storage capacity and the slow movement of subsurface water are manifested as less river runoff in wet season and the subsequent release in dry season, as shown in the mean seasonal river flow in Figure 6b for the four southeastern sub-basins (gauge locations shown in the bottom left panel of Figure 6a, and basin locations in Figure 5b), where LHF produced much reduced seasonal amplitudes in stream discharge than FD, or greater subsurface storage capacity.

[32] At even finer details, we examine the LHF-simulated TWS and its components at the full resolution of the model

(~ 2 km), shown in Figure 7. The subsurface water change clearly dominates (note different color scales for each row), and the northern-southern oscillation of highs and lows follow the Intertropical Convergence Zone. So does the floodwater and river water, but the changes are far smaller and more localized along channels and floodplains.

[33] Lastly, we remark on the interannual variability in TWS. As shown in Figure 4a, the severe drought of 2005 and the wet period of 2009, captured by GRACE observations and discussed in *Chen et al.* [2009a, 2010], are well reproduced by LHF, largely due to its greater subsurface storage capacity that is under-filled during the drought year and over-filled during the pluvial year. Thus, a part of the atmospheric deficit or surplus is absorbed by the subsurface storage. Without sufficient storage capacity, the FD run quickly transfers the deficit or surplus into river discharge, underestimating the hydrologic impacts of atmospheric droughts and pluvial events. Note that the drought of 2010 was weak in the ERA-Interim forcing and hence weakly reflected in the simulated hydrologic response.

6. Summary and Conclusions

[34] In this study, we explored the physical mechanisms whereby groundwater influences terrestrial water storage in the Amazon, using GRACE observations and two model simulations with contrasting versions of the LEAF-Hydro-Flood hydrological model: one with and the other without an interactive groundwater store. Our findings are summarized as below.

[35] First, where the water table is shallow, as found in the northwestern Amazon and the valleys-floodplains elsewhere, subsurface stores are nearly saturated, and surface runoff and flooding dominate the TWS signal. Where the water table is deep and the unsaturated soil

column is substantial, as found in the southeastern Amazon particularly before the wet season, the subsurface storage capacity is large which stores the infiltration and slowly releases it to the streams, and hence the subsurface storage dominates the TWS signal.

[36] Second, over the Amazon as a whole, the enhanced subsurface storage in the southwestern Amazon largely outweighs the reduced subsurface storage in the northwestern Amazon and major floodplains, and as a result, subsurface storage contribution is far greater than surface water contribution to TWS changes. Based on LEAF-Hydro-Flood simulations, 71% of TWS change is due to subsurface water, 24% due to flood water, and 5% due to water confined within river channels.

[37] Third, the subsurface storage has two competing terms, soil water in the vadose zone and groundwater below the water table. As the water table rises and groundwater store grows, it is at the expense of the vadose zone store. Thus, the seasonal response of vadose zone store is directly related to, but in opposite phase with groundwater store.

[38] Our estimates of TWS contributions from different hydrologic stores differ from the earlier estimates without an interactive groundwater, but agree with the findings of Niu *et al.* [2007] that groundwater storage variation explains most of the TWS signal in the Amazon, and of Frappart *et al.* [2011] that subsurface water contributes to ~72% of the TWS change in the downstream reaches of the Rio Negro basin (our estimate: 74%).

[39] In conclusion, we found that both the amplitude and phase of TWS variations in the Amazon are changed when the groundwater dynamics is accounted for in the model, resulting in improved agreement with GRACE measurements, in both amplitude and timing of TWS seasonal variations. The amplitude is increased when groundwater is represented in the model because more water is held during wet seasons and subsequently released during dry seasons. This also results in a considerable time lag in the TWS signal because groundwater acts as a buffer in delaying the response to climate conditions. We found that the variation of subsurface water dominates the variation of TWS when averaged over the entire Amazon basin. However, surface water storages (water in river channels and floodplains) also play a significant role in modulating the variation of TWS in regions where the water table is shallow and seasonal to permanent flooding often occurs.

[40] **Acknowledgments.** Funding comes from NSF-AGS-1045110 and EPA-STAR-RD834190. Computation support comes from CESGA (Centro de Supercomputación de Galicia) Supercomputer Center at the Universidade de Santiago de Compostela, Galicia, Spain, and the Climate Simulation Laboratory at NCAR's Computational and Information Systems Laboratory, sponsored by the National Science Foundation and other agencies. SCH is supported by NASA's Earth Surface and Interior program and GRACE projects.

References

- Alkama, R., B. R. Decharme, H. Douville, M. Becker, A. Cazenave, J. Sheffield, A. Voldoire, S. Tyteca, and P. Le Moigne (2010), Global evaluation of the ISBA-TRIP continental hydrological system. Part I: Comparison with GRACE terrestrial water storage estimates and in situ river discharges, *J. Hydrometeorol.*, *11*, 583–600, doi:10.1175/2010JHM1211.1.
- Alsdorf, D., S.-C. Han, P. Bates, and J. Melack (2010), Seasonal water storage on the Amazon floodplain measured from satellites, *Remote Sens. Environ.*, *114*, 2448–2456, doi:10.1016/j.rse.2010.05.020.
- Bates, P. D., M. S. Horritt, and T. J. Fewtrell (2010), A simple inertial formulation of the shallow water equations for efficient two-dimensional flood inundation modeling, *J. Hydrol.*, *387*, 33–45, doi:10.1016/j.jhydrol.2010.03.027.
- Becker, M., B. Meysignac, L. Xavier, A. Cazenave, R. Alkama, and B. Decharme (2011), Past terrestrial water storage (1980–2008) in the Amazon Basin reconstructed from GRACE and in situ river gauging data, *Hydrol. Earth Syst. Sci.*, *15*, 533–546, doi:10.5194/hess-15-533-2011.
- Betts, A. K., M. Kohler, and Y. Zhang (2009), Comparison of river basin hydrometeorology in ERA-Interim and ERA-40 reanalyses with observations, *J. Geophys. Res.*, *114*, D02101, doi:10.1029/2008JD010761.
- Bongers, F., D. Engelen, and H. Klinge (1985), Phytomass structure of natural plant communities on sodosols in southern Venezuela: The Bana woodland, *Vegetatio*, *63*, 13–34, doi:10.1007/BF00032183.
- Bonnet, M. P., et al. (2008), Floodplain hydrology in an Amazon floodplain lake (Lago Grande de Curuai), *J. Hydrol.*, *349*, 18–30, doi:10.1016/j.jhydrol.2007.10.055.
- Borma, L. S., et al. (2009), Atmosphere and hydrologic controls of the evapotranspiration over a floodplain forest in the Bananal Island region, Amazonia, *J. Geophys. Res.*, *114*, G01003, doi:10.1029/2007JG000641.
- Bourrel, L., L. Phillips, and S. Moreau (2009), The dynamics of floods in the Bolivian Amazon Basin, *Hydrol. Processes*, *23*, 3161–3167, doi:10.1002/hyp.7384.
- Chambers, D. P. (2006), Evaluation of new GRACE time-variable gravity data over the ocean, *Geophys. Res. Lett.*, *33*, L17603, doi:10.1029/2006GL027296.
- Chen, J. L., C. R. Wilson, and B. D. Tapley (2010), The 2009 exceptional Amazon flood and interannual terrestrial water storage change observed by GRACE, *Water Resour. Res.*, *46*, W12526, doi:10.1029/2010WR009383.
- Chen, J. L., C. R. Wilson, and B. D. Tapley (2011), Interannual variability of Greenland ice losses from satellite gravimetry, *J. Geophys. Res.*, *116*, B07406, doi:10.1029/2010JB007789.
- Chen, J. L., C. R. Wilson, B. D. Tapley, Z. L. Yang, and G. Y. Niu (2009a), 2005 drought event in the Amazon River basin as measured by GRACE and estimated by climate models, *J. Geophys. Res.*, *114*, B05404, doi:10.1029/2008JB006056.
- Chen, J. L., C. R. Wilson, D. Blankenship, and B. D. Tapley (2009b), Accelerated Antarctic ice loss from satellite gravity measurements, *Nat. Geosci.*, *2*, 859–862, doi:10.1038/ngeo694.
- Coomes, D. A., and P. J. Grubb (1996), Amazonian caatinga and related communities at La Esmeralda, Venezuela: Forest structure, physiognomy and floristics, and control by soil factors, *Vegetatio*, *122*, 167–191, doi:10.1007/BF00044699.
- Crowley, J. W., J. X. Mitrovica, R. C. Bailey, M. E. Tamisiea, and J. L. Davis (2008), Annual variations in water storage and precipitation in the Amazon Basin, *J. Geodesy*, *82*, 9–13, doi:10.1007/s00190-007-0153-1.
- Cuartas, L. A. (2008), Estudo Observacional E De Modelagem Hidrológica De Uma Micro-Bacia Em Floresta Nao Perturbada Na Amazonia Central, PhD thesis, Inst. Nac. de Pesqui. Espaciais, Sao Jose dos Campos, Brazil.
- Cullmann, J., W. J. Junk, G. Weber, and G. H. Schmitz (2006), The impact of seepage influx on cation content of a Central Amazonian floodplain lake, *J. Hydrol.*, *328*, 297–305, doi:10.1016/j.jhydrol.2005.12.027.
- Duffy, C. J. (1996), A Two-State Integral-Balance Model for Soil Moisture and Groundwater Dynamics in Complex Terrain, *Water Resour. Res.*, *32*, 2421–2434, doi:10.1029/96WR01049.
- Fan, Y., and G. Miguez-Macho (2010), Potential groundwater contribution to Amazon dry-season evapotranspiration, *Hydrol. Earth Syst. Sci.*, *14*, 2039–2056, doi:10.5194/hess-14-2039-2010.
- Fan, Y., G. Miguez-Macho, C. P. Weaver, R. Walko, and A. Robock (2007), Incorporating water table dynamics in climate modeling: 1. Water table observations and the equilibrium water table simulations, *J. Geophys. Res.*, *112*(D10125), doi:10.1029/2006JD008111.
- Forsberg, B. R., A. H. Devol, J. E. Richey, L. A. Martinelli, and H. dos Santos (1988), Factors controlling nutrient concentrations in Amazon floodplain lakes, *Limnol. Oceanogr.*, *33*, 41–56, doi:10.4319/lo.1988.33.1.0041.
- Frappart, F., et al. (2011), Satellite-based estimates of groundwater storage variations in large drainage basins with extensive floodplains, *Remote Sens. Environ.*, *115*, 1588–1594, doi:10.1016/j.rse.2011.02.003.
- Frappart, F., F. Papa, J. S. Famiglietti, C. Prigent, W. B. Rossow, and F. Seyler (2008), Interannual variations of river water storage from a multiple satellite approach: A case study for the Rio Negro River basin, *J. Geophys. Res.*, *113*, D21104, doi:10.1029/2007JD009438.
- Grogan, J., and J. Galvão (2006), Physiographic and floristic gradients across topography in transitional seasonally dry evergreen forests of southeast Para, Brazil, *Acta Amazon.*, *36*, 483–496, doi:10.1590/S0044-59672006000400009.
- Hamilton, S. K., J. Kellndorfer, B. Lehner, and M. Tobler (2007), Remote sensing of floodplain geomorphology as a surrogate for biodiversity in a tropical river system (Madre de Dios, Peru), *Geomorphology*, *89*, 23–38, doi:10.1016/j.geomorph.2006.07.024.

- Han, S.-C., H. Kim, I.-Y. Yeo, P. Yeh, T. Oki, K.-W. Seo, D. Alsdorf, and S. B. Luthcke (2009), Dynamics of surface water storage in the Amazon inferred from measurements of inter-satellite distance change, *Geophys. Res. Lett.*, *36*, L09403, doi:10.1029/2009GL037910.
- Han, S.-C., I.-Y. Yeo, D. Alsdorf, P. Bates, J.-P. Boy, H. Kim, T. Oki, and M. Rodell (2010), Movement of Amazon surface water from time-variable satellite gravity measurements and implications for water cycle parameters in land surface models, *Geochem. Geophys. Geosyst.*, *11*, Q09007, doi:10.1029/2010GC003214.
- Hirschi, M., P. Viterbo, and S. I. Seneviratne (2006), Basin-scale water-balance estimates of terrestrial water storage variations from ECMWF operational forecast analysis, *Geophys. Res. Lett.*, *33*, L21401, doi:10.1029/2006GL027659.
- Hodnett, M. G., I. Vendrame, O. De, A. Marques Filho, M. D. Oyama, and J. Tomasella (1997a), Soil water storage and groundwater behaviour in a catenary sequence beneath forest in central Amazonia: I. Comparisons between plateau, slope and valley floor, *Hydrol. Earth Syst. Sci.*, *1*, 265–277, doi:10.5194/hess-1-265-1997.
- Hodnett, M. G., I. Vendrame, O. De, A. Marques Filho, M. D. Oyama, and J. Tomasella (1997b), Soil water storage and groundwater behaviour in a catenary sequence beneath forest in central Amazonia. II. Floodplain water table behaviour and implications for streamflow generation, *Hydrol. Earth Syst. Sci.*, *1*, 279–290, doi:10.5194/hess-1-279-1997.
- Jirka, S., A. J. McDonald, M. S. Johnson, T. R. Feldpausch, E. G. Couto, and S. J. Riha (2007), Relationships between soil hydrology and forest structure and composition in the southern Brazilian Amazon, *J. Veg. Sci.*, *18*, 183–194, doi:10.1111/j.1654-1103.2007.tb02529.x.
- Johnson, M. S., J. Lehmann, E. C. Selva, M. Abdo, S. Piha, and E. G. Couto (2006), Organic carbon fluxes within and streamwater exports from headwater catchments in the southern Amazon, *Hydrol. Processes*, *20*, 2599–2614, doi:10.1002/hyp.6218.
- Kim, H., P. J.-F. Yeh, T. Oki, and S. Kanae (2009), Role of rivers in the seasonal variations of terrestrial water storage over global basins, *Geophys. Res. Lett.*, *36*, L17402, doi:10.1029/2009GL039006.
- Klees, R., E. A. Zapreeva, H. C. Winsemius, and H. H. G. Savenije (2007), The bias in GRACE estimates of continental water storage variations, *Hydrol. Earth Syst. Sci.*, *11*, 1227–1241, doi:10.5194/hess-11-1227-2007.
- Lähteenoja, O., and S. Page (2011), High diversity of tropical peatland ecosystem types in the Pastaza-Marañón basin, Peruvian Amazonia, *J. Geophys. Res.*, *116*, G02025, doi:10.1029/2010JG001508.
- Landerer, F. W., and S. C. Swenson (2012), Accuracy of scaled GRACE terrestrial water storage estimates, *Water Resour. Res.*, *48*, W04531, doi:10.1029/2011WR011453.
- Lesack, L. F. W. (1993), Water balance and hydrologic characteristics of a rain forest catchment in the central Amazon Basin, *Water Resour. Res.*, *29*, 759–773, doi:10.1029/92WR02371.
- Lesack, L. F. W. (1995), Seepage exchange in an Amazon floodplain lake, *Limnol. Oceanogr.*, *40*, 598–609, doi:10.4319/lo.1995.40.3.0598.
- Lesack, L. F. W., and J. M. Melack (1995), Flooding hydrology and mixture dynamics of lake water derived from multiple sources in an Amazon floodplain lake, *Water Resour. Res.*, *31*, 329–345, doi:10.1029/94WR02271.
- Lo, M.-H., J. S. Famiglietti, P. J.-F. Yeh, and T. H. Syed (2010), Improving parameter estimation and water table depth simulation, in a land surface model using GRACE water storage and estimated baseflow data, *Water Resour. Res.*, *46*, W05517, doi:10.1029/2009WR007855.
- Luthcke, S. B., D. D. Rowlands, F. G. Lemoine, S. M. Klosko, D. Chinn, and J. J. McCarthy (2006), Monthly spherical harmonic gravity field solutions determined from GRACE inter-satellite range-rate data alone, *Geophys. Res. Lett.*, *33*, L02402, doi:10.1029/2005GL024846.
- Mason, B. G., D. M. Pyle, W. B. Dade, and T. Jupp (2004), Seasonality of volcanic eruptions, *J. Geophys. Res.*, *109*, B04206, doi:10.1029/2002JB002293.
- McClain, M. E., J. E. Richey, and J. A. Brandes (1997), Dissolved organic matter and terrestrial-lotic linkages in the central Amazon basin of Brazil, *Global Biogeochem. Cycles*, *11*, 295–311, doi:10.1029/97GB01056.
- Mertes, L. A. K. (1997), Documentation and significance of the perirheic zone on inundated floodplains, *Water Resour. Res.*, *33*, 1749–1762, doi:10.1029/97WR00658.
- Miguez-Macho, G., and Y. Fan (2012a), The role of groundwater in the Amazon water cycle: 1. Influence on seasonal streamflow, flooding and wetlands, *J. Geophys. Res.*, *117*, D15113, doi:10.1029/2012JD017539.
- Miguez-Macho, G., and Y. Fan (2012b), The role of groundwater in the Amazon water cycle: 2. Influence on seasonal soil moisture and evapotranspiration, *J. Geophys. Res.*, *117*, D15114, doi:10.1029/2012JD017540.
- Miguez-Macho, G., Y. Fan, C. P. Weaver, R. Walko, and A. Robock (2007), Incorporating water table dynamics in climate modeling: 2. Formulation, validation, and simulations of soil moisture fields, *J. Geophys. Res.*, *112*(D13108), doi:10.1029/2006JD008112.
- Neu, V., C. Neill, and A. V. Krusche (2011), Gaseous and fluvial carbon export from an Amazon forest watershed, *Biogeochemistry*, *105*, 133–147, doi:10.1007/s10533-011-9581-3.
- Ngo-Duc, T., K. Laval, G. Ramillien, J. Polcher, and A. Cazenave, Validation of the land water storage simulated by organising carbon and hydrology in dynamic ecosystems (orchidee) with gravity recovery and climate experiment (GRACE) data (2007), *Water Resour. Res.*, *43*, W04427, doi:10.1029/2006WR004941.
- Niu, G.-Y., and Z.-L. Yang (2006), Assessing a land surface model's improvements with GRACE estimates, *Geophys. Res. Lett.*, *33*, L07401, doi:10.1029/2005GL025555.
- Niu, G.-Y., Z.-L. Yang, R. E. Dickinson, L. E. Gulden, and H. Su (2007), Development of a simple groundwater model for use in climate models and evaluation with Gravity Recovery and Climate Experiment data, *J. Geophys. Res.*, *112*, D07103, doi:10.1029/2006JD007522.
- Poels, R. L. H. (1987), *Soils, Water and Nutrients in a Forest Ecosystem in Suriname*, Agric. Univ. at Wageningen, Wageningen, Netherlands.
- Pokhrel, Y., N. Hanasaki, S. Koirala, J. Cho, H. Kim, P. J.-F. Yeh, S. Kanae, and T. Oki (2012), Incorporating anthropogenic water regulation modules into a land surface model, *J. Hydrometeorol.*, *13*, 255–269, doi:10.1175/JHM-D-11-013.1.
- Rodell, M., and J. S. Famiglietti (2002), The potential for satellite-based monitoring of groundwater storage changes using GRACE: The High Plains aquifer, central, U.S., *J. Hydrol.*, *263*(1–4), 245–256.
- Rodell, M., J. S. Famiglietti, J. Chen, S. I. Seneviratne, P. Viterbo, S. Holl, and C. R. Wilson (2004), Basin scale estimates of evapotranspiration using GRACE and other observations, *Geophys. Res. Lett.*, *31*, L20504, doi:10.1029/2004GL020873.
- Schaller, M. F., and Y. Fan (2009), River basins as groundwater exporters and importers: Implications for water cycle and climate modeling, *J. Geophys. Res.*, *114*, D04103, doi:10.1029/2008JD010636.
- Selhorst, D., S. A. Vieira, and I. F. Brown (2003), Agua e crescimento de uma floresta na Amazonia Sul-Occidental, Acre, Brasil: Chuva afeta crescimento, mas nível do lençol freático não, poster report, Univ. Fed. do Acre, Rio Branco, Brazil. [ftp://lba.cptec.inpe.br/lba_archives/LC/LC-02/Posters/SelhorstDiogo Poster VI CEB 02nov03.pdf.]
- Seo, K.-W., C. R. Wilson, J. S. Famiglietti, J. L. Chen, and M. Rodell (2006), Terrestrial water mass load changes from Gravity Recovery and Climate Experiment (GRACE), *Water Resour. Res.*, *42*, W05417, doi:10.1029/2005WR004255.
- Swenson, S., J. Wahr, and P. C. D. Milly (2003), Estimated accuracies of regional water storage variations inferred from the Gravity Recovery and Climate Experiment (GRACE), *Water Resour. Res.*, *39*(8), 1223, doi:10.1029/2002WR001808.
- Syed, T. H., J. S. Famiglietti, M. Rodell, J. Chen, and C. R. Wilson (2008), Analysis of terrestrial water storage changes from GRACE and GLDAS, *Water Resour. Res.*, *44*, W02433, doi:10.1029/2006WR005779.
- Tapley, B. D., S. Bettadpur, J. C. Ries, P. F. Thompson, and M. M. Watkins (2004), GRACE measurements of mass variability in the Earth system, *Science*, *305*, 503–505, doi:10.1126/science.1099192.
- Tomasella, J., M. G. Hodnett, L. A. Cuartas, A. D. Nobre, M. J. Waterloo, and S. M. Oliveira (2008), The water balance of an Amazonian microcatchment: The effect of interannual variability of rainfall on hydrological behavior, *Hydrol. Processes*, *22*, 2133–2147, doi:10.1002/hyp.6813.
- Toth, J. (1963), A theoretical analysis of groundwater flow in small drainage basins, *J. Geophys. Res.*, *68*, 4795–4812.
- Vourlitis, G. L., J. D. Nogueira, F. D. Lobo, K. M. Sendall, S. R. de Paulo, C. A. A. Dias, O. B. Pinto Jr., and N. L. R. de Andrade (2008), Energy balance and canopy conductance of a tropical semi-deciduous forest of the southern Amazon Basin, *Water Resour. Res.*, *44*, W03412, doi:10.1029/2006WR005526.
- Wahr, J., S. Swenson, V. Zlotnicki, and I. Velicogna (2004), Timevariable gravity from GRACE: First results, *Geophys. Res. Lett.*, *31*, L11501, doi:10.1029/2004GL019779.
- Walko, R. L., et al. (2000), Coupled atmosphere-biophysics-hydrology models for environmental modeling, *J. Appl. Meteorol.*, *39*, 931–944, doi:10.1175/1520-0450(2000)039<0931:CABHMF>2.0.CO;2.
- Werth, S. and A. Güntner (2010), Calibration analysis for water storage variability of the global hydrological model WGHM, *Hydrol. Earth Syst. Sci.*, *14*, 59–78, doi:10.5194/hess-14-59-2010.
- Winter, T. C., J. W. Harvey, O. L. Franke, and W. A. Alley (1998), Ground water and surface water: A single resource, *U.S. Geol. Surv. Circ.*, *1139*, 79.
- Xavier, L., M. Becker, A. Cazenave, L. Longuevergne, W. Llovel, and O. C. Rotunno Filho (2010), Interannual variability in water storage over 2003–2008 in the Amazon basin from GRACE space gravimetry, in situ river level and precipitation data, *Remote Sens. Environ.*, *114*, 1629–1637, doi:10.1016/j.rse.2010.02.005.
- Yamazaki, D., S. Kanae, H. Kim, and T. Oki (2011), A physically based description of floodplain inundation dynamics in a global river routing model, *Water Resour. Res.*, *47*, W04501, doi:10.1029/2010WR009726.
- Yeh, P., S. Swenson, J. Famiglietti, and M. Rodell (2006), Remote sensing of groundwater storage changes in Illinois using the gravity recovery and climate experiment (GRACE), *Water Resour. Res.*, *42*, W12203, doi:10.1029/2006WR005374.